Augmentation of Checkpoint Inhibitor Tumor Response via Adjuvant Cryoablation in Murine Lung, Breast and Colon Cancer Models

Scholarly Report submitted in partial fulfillment of the MD Degree at Harvard Medical School

Date: 31 March 2018

Student Name: Perry John Hampilos

Scholarly Report Title: Augmentation of checkpoint inhibitor tumor response via adjuvant cryoablation in murine lung, breast and colon cancer models.

Mentor Name and Affiliations: Umar Mahmood, MD PhD, Imaging Division, Massachusetts General Hospital

Collaborators, with Affiliations: Eric Wehrenberg-Klee, MD, Massachusetts General Hospital and Benjamin Larimer, PhD, Massachusetts General Hospital

Abstract

TITLE: Augmentation of checkpoint inhibitor tumor response via adjuvant cryoablation in murine lung, breast and colon cancer models.

Perry Hampilos, BA, Eric Wehrenberg-Klee, MD, Benjamin Larimer, PhD and Umar Mahmood, MD PhD

Purpose: Focal cryoablation for cancer is an immunogenic process that can also result in a global antitumor response. We hypothesize that combining cryoablation with immunotherapy will yield an augmented synergistic antitumor response in syngenic murine tumor models.

Methods: Mice were implanted with bilateral flank tumors of lung, breast or colon cancer and were treated with checkpoint inhibitor therapy (anti-PD-1/anti-CTLA-4) and/or unilateral cryoablation. Tumor volumes were measured for up to 4 weeks to track growth delay, and survival analysis was performed with an endpoint of tumor volume >750mm^3.

Results: The lung cancer model did not demonstrate growth delay or survival benefit to immunotherapy, cryoablation, or both compared to vehicle. The colon cancer model was sensitive to immunotherapy regimens, with both groups demonstrating growth delay and improved survival; the addition of cryoablation to immunotherapy resulted in improved survival compared to immunotherapy alone, as well as complete tumor regression in 80% of cases. The breast cancer model was partially responsive to immunotherapy, which resulted in a growth delay and improved survival; again this response was improved by cryoablation over immunotherapy alone, however no complete tumor regression was observed.

Conclusions: Checkpoint inhibitors are a potent yet cancer type-dependent therapy. The antitumor immune response can be augmented by the combination of immunotherapy with focal cryoablation.

Table of Contents

Glossary of abbreviations

IO – immunotherapy (anti-PD-1/anti-CTLA-4)

LLC1 – murine Lewis lung carcinoma cell line

EMT6 – murine breast mammary carcinoma cell line

MC38 – murine colon carcinoma cell line

Introduction

The immune system has long been implicated in the pathogenesis of cancer; inflammatory and immune responses are known to play roles in both oncogenesis and tumor suppression. More recently, the field of immuno-oncology has harnessed the latter as an angle of attack on aggressive or resistant cancers. Clinical responses have been demonstrated in metastatic melanoma, triple negative breast cancer, non-small cell lung cancer and others. Checkpoint inhibitors, such as pembrolizumab (anti PD-1) or ipilimumab (anti CTLA-4), are a subgroup of immunotherapy, which use antibodies to target surface molecules that inhibit T-cell activation. The normal roles of PD-1/CTLA-4 are to recognize host cells and suppress potential autoimmune responses. However this mechanism can be coopted by cancer cells in order to evade the host tumor immune response. By inhibiting the checkpoint on T-cell activation, checkpoint inhibitors stimulate a more robust immune response to cancer antigens, while also increasing the risk of various autoimmune side effects.[1]

While traditional chemotherapeutic agents have general immunosuppressive effects, targeted radiation and ablative therapies have the ability to induce a tumor immune response by increasing tumor antigen exposure to the immune system. These therapies cause tissue injury, specifically cell necrosis, and local inflammation, which expose “foreign” tumor antigens to activated immune cells.[2] Cryoablation is a particularly immunogenic therapy, as it not only induces necrosis, but also avoids denaturation of released antigens.[3] By exposing these abnormal proteins, focal therapy can induce a global humoral/cellular immune response against both primary and metastatic lesions. This clinical response to focal treatment is known as the abscopal effect. The abscopal effect is predominantly associated with radiation therapy, however it has been reported with ablation therapy as well. The mechanism behind the abscopal effect is thought to be immune, with the specific pathways still under investigation.[4] Unfortunately, this powerful effect is also inconsistent and occurs in a minority of cases. However, the advent of modern immune-therapy has opened the possibility of combining an immunogenic focal therapy with checkpoint inhibitors to unleash the immune system and elicit an augmented and lasting host tumor immune response.[5,6]

The objective of this study is to characterize the immune response of checkpoint inhibitor therapy and cryoablation therapy and to evaluate the efficacy of individual and combination therapy. This work will build on previous studies demonstrating synergistic effects of combining focal ablation therapy with checkpoint inhibitors. Murine lung (LLC1), breast (EMT6) and colon (MC38) carcinoma cell lines were selected for testing in syngenic mice. Our hypothesis is that combination therapy will augment the

tumor immune response and induce an abscopal effect, resulting in a robust global anti-tumor response and improved survival over either therapy alone.

Student role

I was involved with experiment design and planning, and conducted the majority of bench work, animal studies and data analysis. I worked and conferred with other senior lab members and several research assistants/technicians. This work was completed in Dr. Umar Mahmood's basic science laboratory at the MGH Navy Yard campus in Charlestown, MA. We have no collaborations for this project at this time.

Methods

Animals

All experiments were approved by and conducted in accordance to the Massachusetts General Hospital Institutional Animal Care and Use Committee. 8 – 12 week old female BALB/c white mice and C57BL/6 black mice were acquired from Charles River (Massachusetts, USA). Mice were housed in cages in a climate/light cycle controlled animal room.

Cell culture

Cells were cultured on tissue culture plates and housed in a humidified 37°C 5% CO_2 incubator. LLC1 and MC38 cells were cultured in DMEM medium (Gibco) supplemented by 10% fetal bovine serum. EMT6 cells were cultured in Waymouth's medium (Gibco) supplemented by 15% FBS. Cells were routinely split when subconfluent using TrypLE (Gibco).

Tumor models

Tumors injections were prepared at 5 x 10^6 cells/mL concentration in a 1:1 medium to Matrigel (Corning) suspension in a 1cc syringe with 25G hypodermic needle and kept on ice. Mice were anesthetized using continuous isoflurane gas and injected subcutaneously in the dorsolateral upper flank regions. Each tumor injection had a volume of 100uL containing 5 x 10^5 cells/tumor. Tumors were measured starting day 3-4 post implantation, followed by every 2-3 days thereafter, and tumor volumes were calculated using the formula: volume = 3.14 x length x $(0.5 \times \text{width})^2$. Mice were sacrificed for high tumor burden, tumor ulceration or veterinary concern.

Immunotherapy

Immunotherapy regimen included anti-mouse PD-1 (clone RMP1-14, Bio X Cell, West Lebanon, NH) and/or anti-mouse CTLA-4 (clone 9H10, Bio X Cell, West Lebanon, NH) intraperitoneal injections at 200 and 100 ug/injection respectively, and was administered in three doses on days 3,6,9 or 2,5,8 post implantation.

Ablation

Cryoablation was performed once on days 8-11 using a pressurized liquid nitrogen canister with nozzle applicator. Mice were anesthetized under continuous isoflurane on warming plates. The skin adjacent to the tumor was shaved, sterilized and opened via a 10mm incision to expose the right flank tumor. Liquid nitrogen was applied at a distance of 5mm for two freezing cycles of 30 seconds split by a 120 second thaw cycle, with the goal of estimated 50% tumor ablation. The incision was approximated and closed by sterile surgical staples.

Data analysis

Clinical response to therapy was analyzed through individual tumor growth curves, group mean +/- SEM, and Kaplan-Meier survival plots. Means were compared using student's t-test, with $p<0.05$ defined as statistical significance. Ulcerated tumor measurements were excluded. Measurements of the ablated tumors were also excluded. The primary endpoint for Kaplan-Meier survival plots was defined as measured tumor volume >750mm^3, and complete tumor regression was defined as consecutive final measurements of <7mm^3. Mice in the ablation groups that did not undergo ablation were excluded from the analysis.

Results

Unilateral tumor model development

Prior studies of syngeneic MC38 colon carcinoma mouse models had demonstrated a robust response to anti-PD-1/anti-CTLA-4 immunotherapy (data not shown). To better demonstrate the effects of adding cryoablation to immunotherapy, additional syngeneic tumor models were developed, with the goal of a spectrum of responsiveness to immunotherapy and/or ablation. LLC1 lung carcinoma and EMT6 breast carcinoma cells were selected as potential aggressive and less responsive tumor models. In the initial LLC1 unilateral tumor models there was no observed growth delay between the vehicle and IO groups (figure 2A). In the EMT6 unilateral tumor models, immunotherapy appeared to confer a growth delay within the first two weeks (figure 2B), however this effect was not statistically significant. These models were selected as challenging targets for a more aggressive combination of immunotherapy and cryoablation.

Bilateral tumor model development

In order to observe the abscopal effect in mice undergoing cryoablation, it was necessary to develop a metastatic tumor model. Mice underwent bilateral implantation of tumors, with the right tumor scheduled for cryoablation and the left tumor measured to evaluate global effects of the contralateral focal therapy (figure 1). The LLC1 tumors were again the least responsive to immunotherapy, as well as cryoablation or IO/ablation (figure 3A). On days 14 and 16 post implantation, there was no statistical significance between the vehicle and any treatment group. Furthermore, there was no observable survival benefit in any of the treatment groups (figure 3B).

In contrast, the MC38 bilateral tumor model was the most responsive to immunotherapy. Despite the increased tumor burden, mice treated with immunotherapy demonstrated significant and persistent growth delays by day 10 in the IO group, and day 12 in the IO/ablation group. Cryoablation therapy alone did not yield any significant growth delay. Comparison of the IO and IO/ablation groups during the first 14 days post implantation appeared to demonstrate a greater growth delay in the IO/ablation group, however this was not statistically significant during this timeframe (figure 4A). However, four of five mice in the IO/ablation group experienced complete tumor regression after day 16, compared with only one of five in the IO alone group (supplemental data B). Kaplan-Meier survival plots demonstrated a marked survival benefit of at least 14 days in the IO groups over the vehicle and ablation groups (figure 4B).

The EMT6 tumor model fell in the middle of the responsiveness spectrum, as suggested by the initial unilateral tumor data. Similar to the previous two models, cryoablation alone did not yield any growth delay compared to the vehicle groups. Within the first two weeks, significant and persistent growth delays were observed in the IO (days 3,6,9) +/- ablation groups, as well as the IO (days 2,5,8) +/- ablation groups (the advanced immunotherapy regimen starting on day 2 post implantation was attempted as a more aggressive treatment). During the first two week period, there was no statistically significant difference between the immunotherapy alone and the immunotherapy/ablation groups. Kaplan-Meier survival plots did demonstrate a survival benefit in the combination therapy groups over the immunotherapy alone group, extending survival by 2-4 days. While most of the cryoablation alone mice reached the study endpoint by day 16, a single mouse did have the longest overall survival time.

Discussion

These initial trials demonstrate the potential in combining checkpoint inhibitor immunotherapy with focal cryoablation to achieve a synergistic global tumor immune response. In the MC38 model, the addition of cryoablation augmented an already strong tumor growth delay response to immunotherapy alone, achieving complete tumor regression in 80% of the mice. This robust response was not unilaterally shared by the other models and appeared to be cell line dependent, as the LLC1 models were entirely unresponsive and the EMT6 models were only partially responsive. While differences in tumor aggressiveness (untreated tumor growth rate) may be a factor, all three cell lines demonstrated comparable growth rates and survival endpoints in the vehicle groups. It is more likely that the molecular phenotype of the cells with respect to checkpoint inhibitor targets contributed to this difference, as cellular methods to evade the natural antitumor immune response differ among cancers. One would hypothesize that the MC38 colon cancer cells are more reliant on PD-1 and CTLA-4 expression to evade the host immune response, and thus would be more susceptible to those checkpoint inhibitor therapies. While our clinical data demonstrates that responsiveness to immunotherapy alone was necessary for an augmented response from combined immunotherapy/cryoablation, this phenomenon needs to be further studied through biochemical techniques. Characterizing the tumor immune marker expression profiles will not only test this hypothesis, but also identify other targets for immunotherapy beyond PD-1 and CTLA-4.

It is also possible that while the therapies are correct, the treatment regimen and parameters must be adjusted to elicit an improved response. A focus of future study will be in evaluating the parameters of cryoablation, including the duration, target temperature and size of the ablation area, as well as the tumor size or day post implantation when the ablation is performed. Lastly, the timing of immunotherapy with respect to ablation may impact the resultant immune response; comparing neoadjuvant regimens in this study to adjuvant regimens is will be the subject of future trials.

Limitations of this study include a limited sample size, which lacked the power in some instances to show statistical significance of observed potential effects, most notably in determining the effect of combining cryoablation with immunotherapy on tumor growth. Nonetheless, the synergistic effect of the combination was well represented in survival. This might also suggest that combination therapy does not significantly affect early tumor growth but does improve long-term survival through a delayed antitumor response. This distinction will be important to elucidate, as if early growth delay is indeed an indicator of long-term survival, tumors demonstrating growth delay could be excised at early time points to investigate the cellular and molecular mechanisms of the antitumor immune response/abscopal effect, using immunohistochemistry, flow cytometry and other techniques that unfortunately destroy the tumor in the process. These studies would help to reveal the mechanisms of successful vs unsuccessful antitumor immune responses. Alternatively, our group has developed a granzyme PET-tracer probe that has been used to image local immune activity in live mice via PET-CT/MRI. It is conceivable that this novel technology could be applied to non-invasively observe the ability of immunotherapy and cryoablation to induce immune cell infiltration and activation in the tumors and identify predictors of a successful response.[7,8]

Most excitingly, this work has the potential to advance the field of cancer immunotherapy by enhancing already established therapeutic modalities. Ablation and immunotherapy are already well incorporated into the oncology arsenal for a multitude of human cancers. The study of individual mechanisms of action and optimal cancer specific protocols in mouse models will advance the development of powerful therapeutic regimens that take advantage of the anti-tumor immune response through checkpoint inhibition and increased antigen presentation, regimens we hope may ultimately translate to the clinic in the near future.

Acknowledgements

This work was contributed to by Emily Austin and Sarah Nesti of the Mahmood Lab.

References

1) Khalil DN, Smith EL, Brentjens RJ, Wolchok JD. The future of cancer treatment: immunomodulation, CARs and combination immunotherapy. Nature Reviews Clinical Oncology. 2016;13(5):273-90.
2) Weichselbaum RR, Liang H, Deng L and Fu YX. Radiotherapy and immunotherapy: a beneficial liaison? Nature Reviews Clinical Oncology. 2017;14(6):365-79.
3) Sabel MS. Cryo-immunology: a review of the literature and proposed mechanisms for stimulatory versus suppressive immune responses. Cryobiology. 2009;58:1–11.
4) Slovak R, Ludwig JM, Gettinger SN, Herbst RS, Kim HS. Immuno-thermal ablations – boosting the anticancer immune response. Journal for ImmunoTherapy of Cancer. 2017;5(78):1-15.
5) Tang C, Wang X, Soh H, Seyedin S, Cortez MA, Krishnan S, Massarelli E, Hong D, Naing A, Diab A, Gomez D, Huiping Y, Heymach J, Komaki R, Allison J, Sharma P and Welsh J. Combining radiation and immunotherapy: a new systemic therapy for solid tumors?. Cancer Immunol Res. 2014 September;2(9):831-8.
6) Benzon B, Glavaris SA, Simons BW, Hughes RM, Ghabili K, Mullane P, Miller R, Nugent K, Shinder B, Tosoian J, Fuchs EJ, Tran PT, Hurley PJ, Vuica-Ross M, Schaeffer EM, Drake CG, and Ross AE. Combining immune check-point blockade and cryoablation in an immunocompetent hormone sensitive murine model of prostate cancer. Springer Nature: Prostate Cancer and Prostatic Diseases. 20 Mar 2018. online.
7) Larimer BM, Wehrenberg-Klee EP, Dubois F, Mehta A, Kalomeris T, Flaherty K, Boland G, and Mahmood U. Granzyme B PET imaging as a predictive biomarker of immunotherapy response. Cancer Research. 2017;77(9):2318-27.
8) Larimer BM, Wehrenberg-Klee EP, Caraballo A and Mahmood U. Quantitative CD3 PET imaging predicts tumor growth response to anti-CTLA-4 therapy. Journal of Nuclear Medicine. 2016;57(10):16070-11.

Figure 1: Schematic on bilateral tumor model development and immunotherapy/cryoablation treatment regimens.

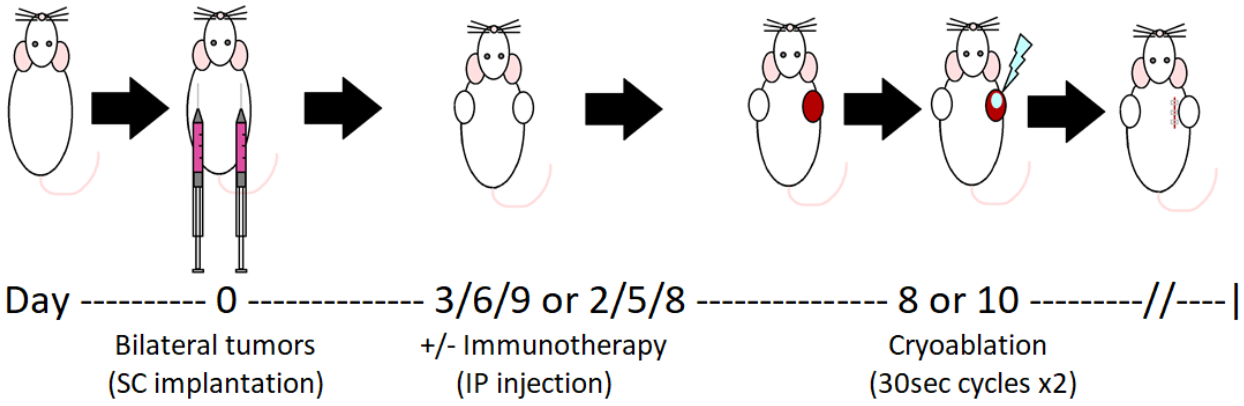

1A) Mice are injected with 5 x 10^5 cells in suspension matrix in right and left upper dorsal flanks on day 0, and measured every 2-4 days. Immunotherapy groups receive intraperitoneal injections of anti-PD-1 and anti-CTLA-4 on days 3,6,9 or 2,5,8 post implantation. Cryoablation groups undergo two cycles of ~50% ablation on day 8 or 10 post implantation.

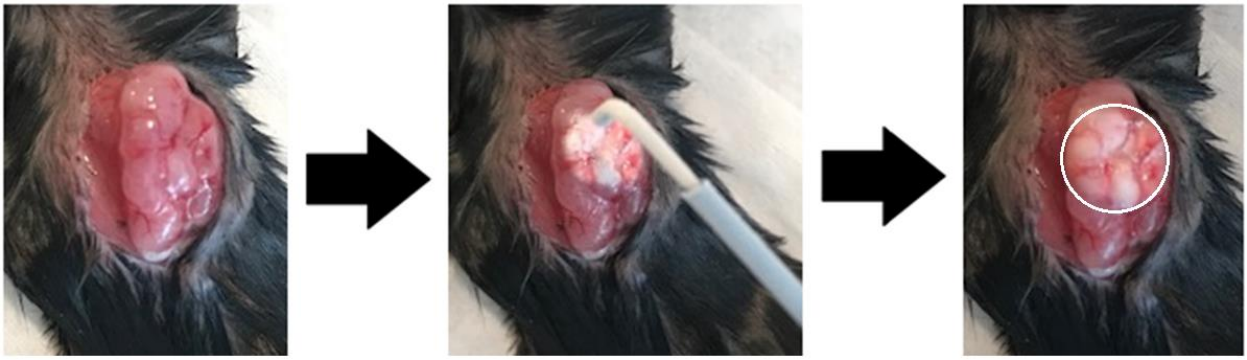

1B) Images of cryoablation procedure. The skin adjacent to the right flank tumor is opened to expose the tumor. Pressurized liquid nitrogen is applied for two 30 second freeze cycles separated by a 120 second thaw cycle to achieve ~50% tumor ablation, visualized by a white frozen area (white circle).

Figure 2: Unilateral tumor model development to assess immunotherapy on tumor growth

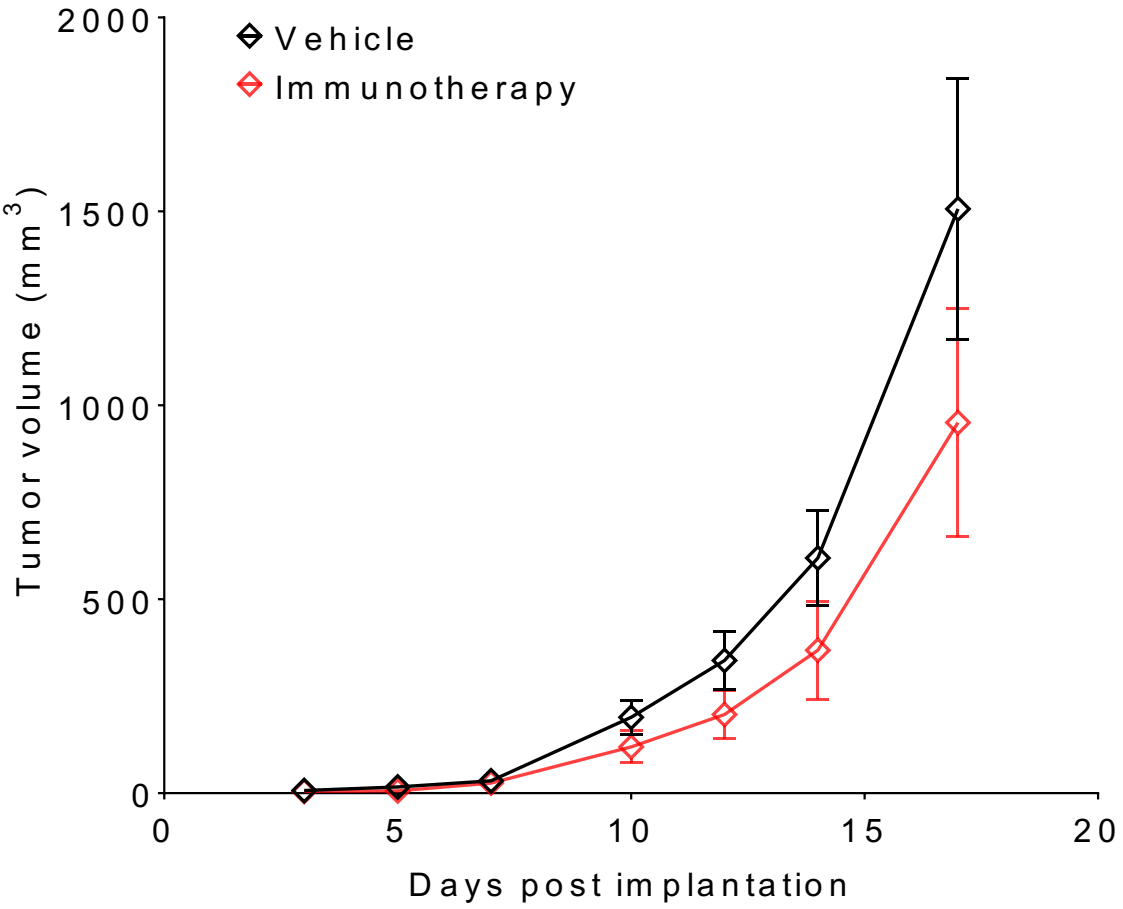

2A) LLC1 growth curves for vehicle (n = 5) and immunotherapy (n = 5) groups, plotted as group mean +/- SEM. P values for day 12 (p = 0.19), day 14 (p = 0.21), and day 17 (p = 0.25).

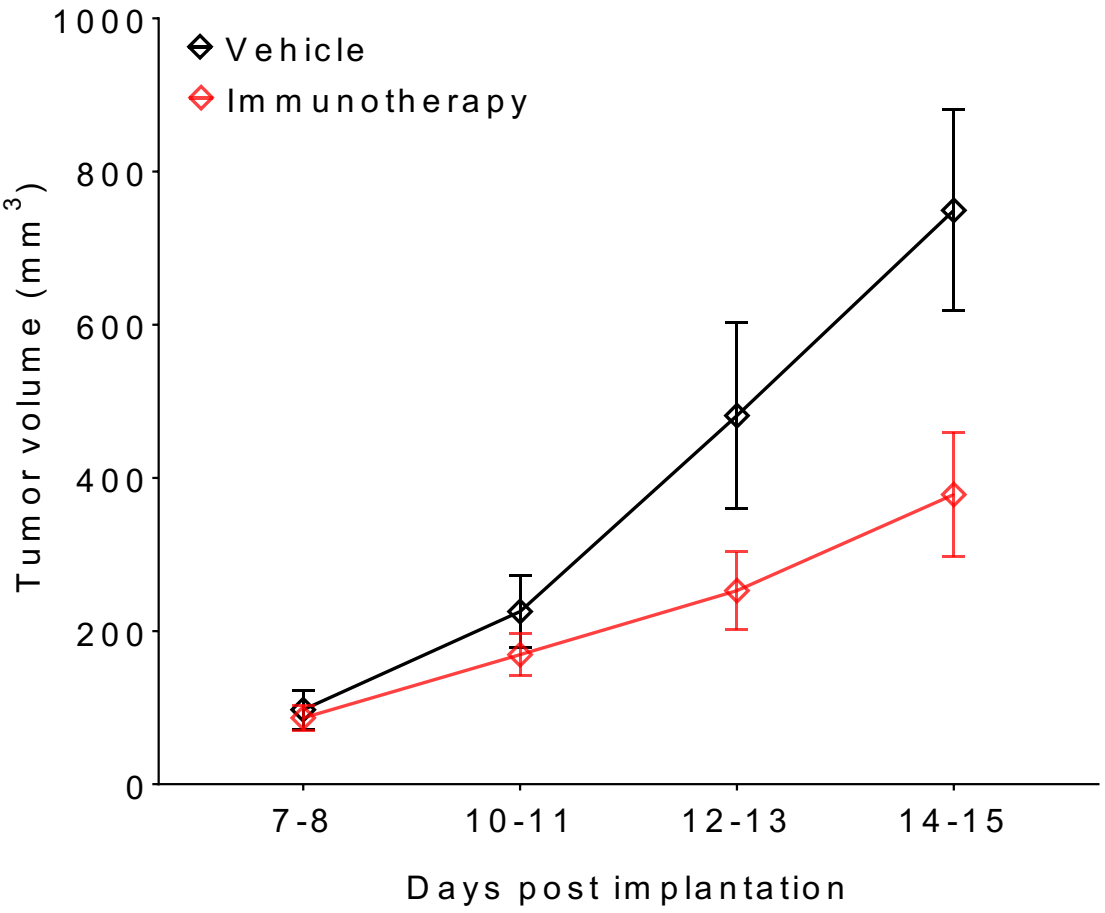

2B) EMT6 growth curves for vehicle (n = 5) and immunotherapy (n = 5) groups, plotted as group mean +/- SEM. P values for day 10 (p = 0.50), day 12 (p = 0.22), and day 14 (p = 0.10).

Figure 3: LLC1 bilateral tumor model development to assess immunotherapy and/or cryoablation on tumor growth.

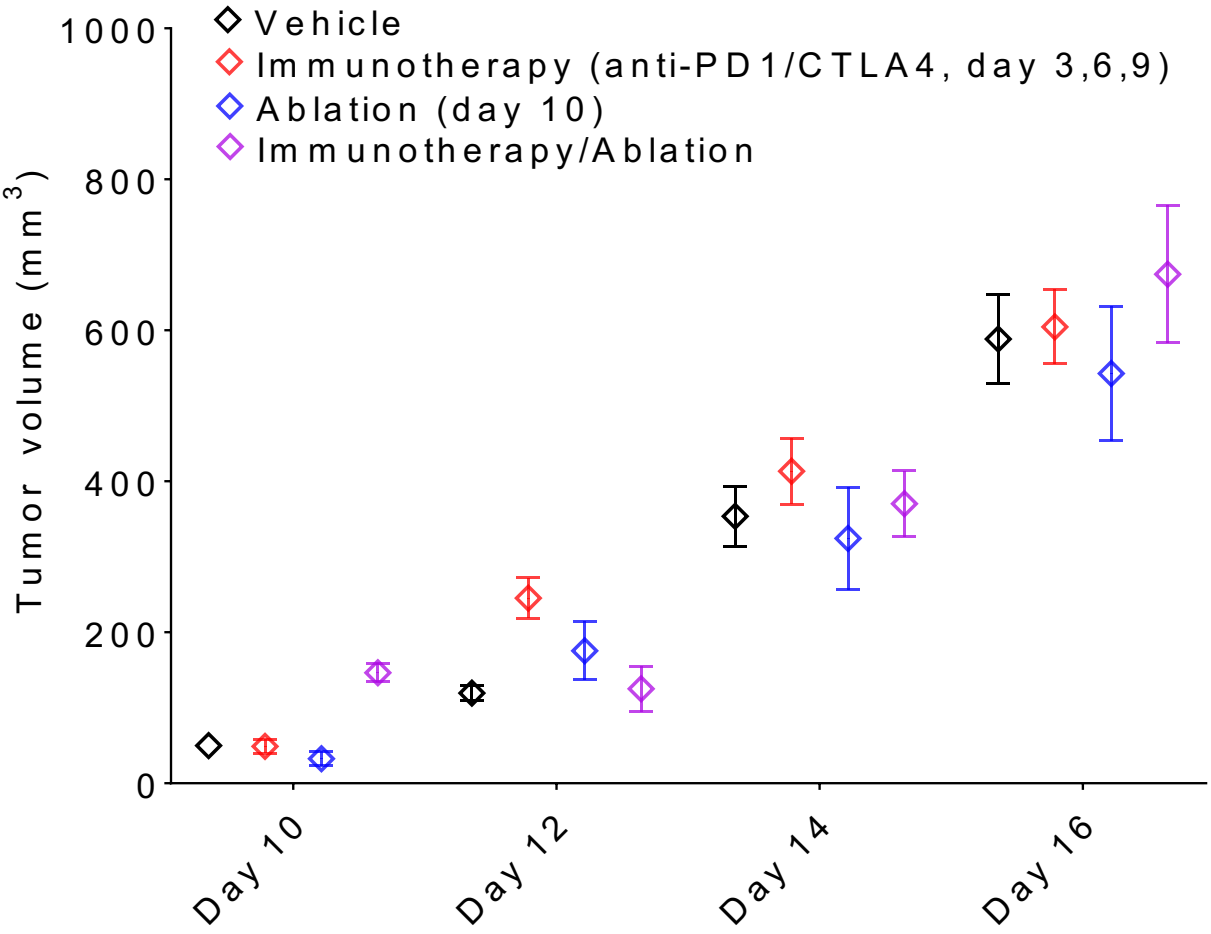

3A) LLC1 growth curves for vehicle (n = 8), immunotherapy (n= 8), ablation (n = 8) and combination (n = 9) groups, plotted as group mean +/- SEM. P values for vehicle vs IO for day 10 (p = 0.95), day 12 (p = 0.0001), day 14 (p = 0.33), and day 16 (p = 0.83). P values for vehicle vs ablation for day 10 (p = 0.23), day 12 (p = 0.08), day 14 (p = 0.69), and day 16 (p = 0.66). P values for vehicle vs IO/ablation for day 10 (p = 0.000001), day 12 (p = 0.82), day 14 (p = 0.78), and day 16 (p = 0.41).

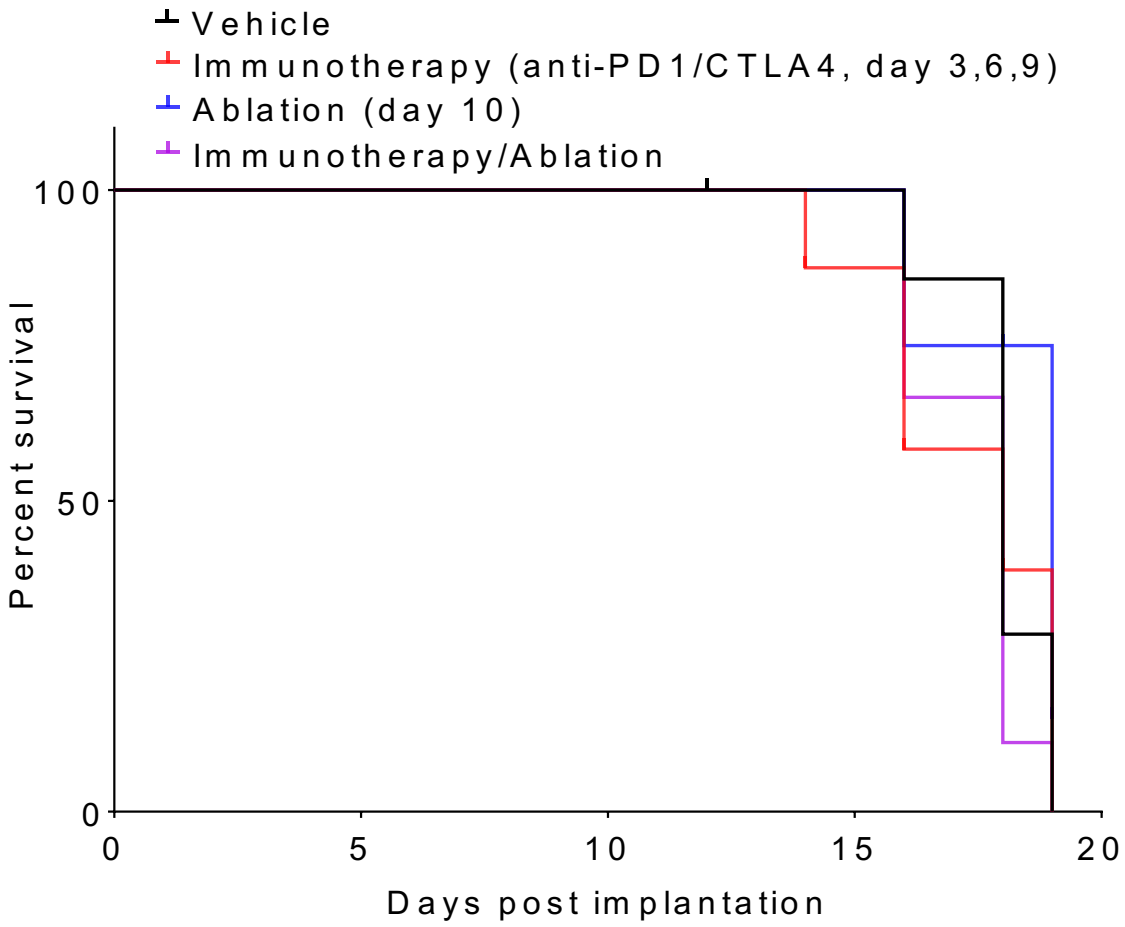

3B) Kaplan-Meier survival plots of LLC1 mice with bilateral tumors. Endpoint defined as tumor volume > 750mm^3.

Figure 4: MC38 bilateral tumor model development to assess immunotherapy and/or cryoablation on tumor growth.

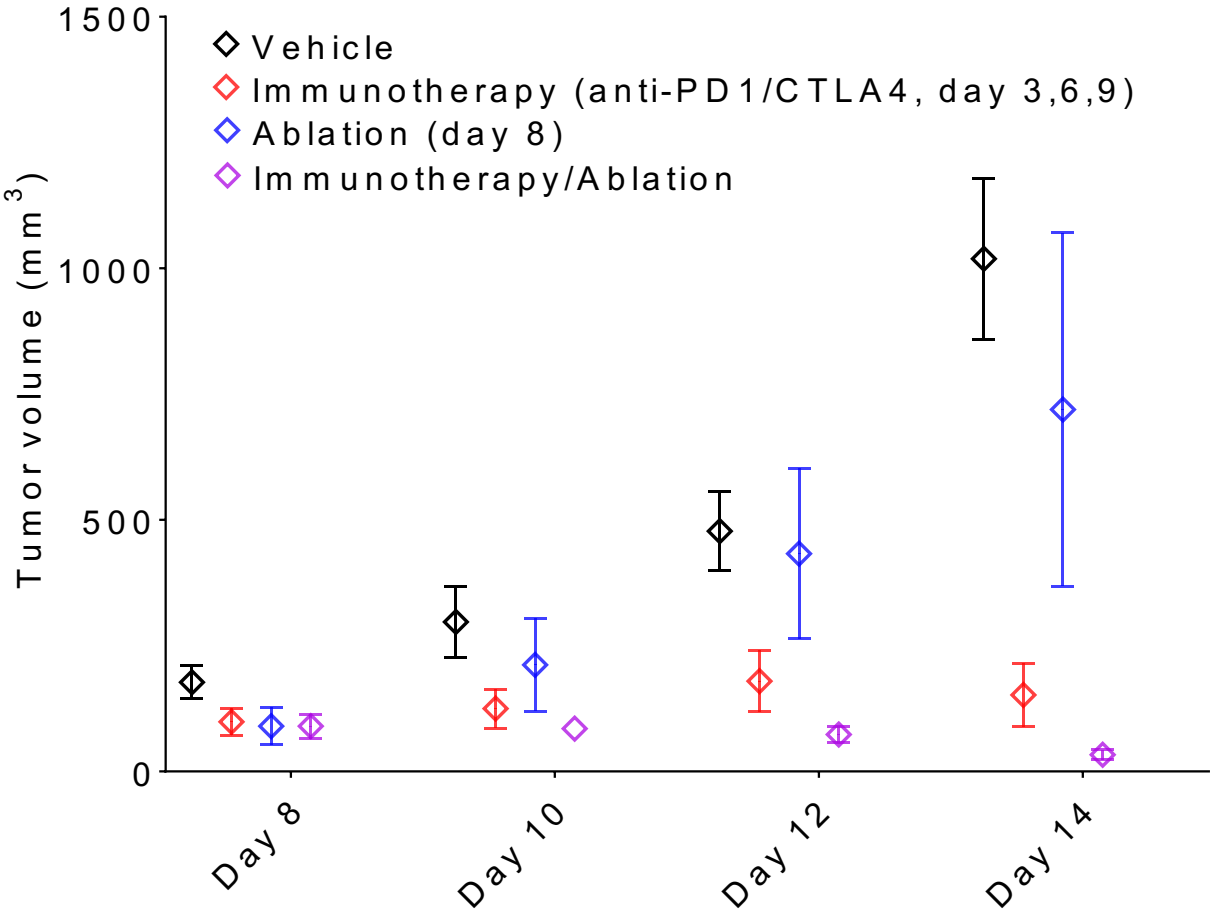

4A) MC38 growth curves for vehicle (n = 5), immunotherapy (n= 5), ablation (n = 5) and combination (n = 5) groups plotted as group mean +/- SEM. P values for vehicle vs IO for day 8 (p = 0.07), day 10 (p = 0.05), day 12 (p = 0.008), and day 14 (p = 0.00009). P values for vehicle vs ablation for day 8 (p = 0.12), day 10 (p = 0.49), day 12 (p = 0.79), and day 14 (p = 0.39). P values for vehicle vs IO/ablation for day 8 (p = 0.10), day 10 (p = 0.06), day 12 (p = 0.004), and day 14 (p = 0.0009). P values for IO vs IO/ablation for day 8 (p = 0.84), day 10 (p = 0.50), day 12 (p = 0.26), and day 14 (p = 0.21).

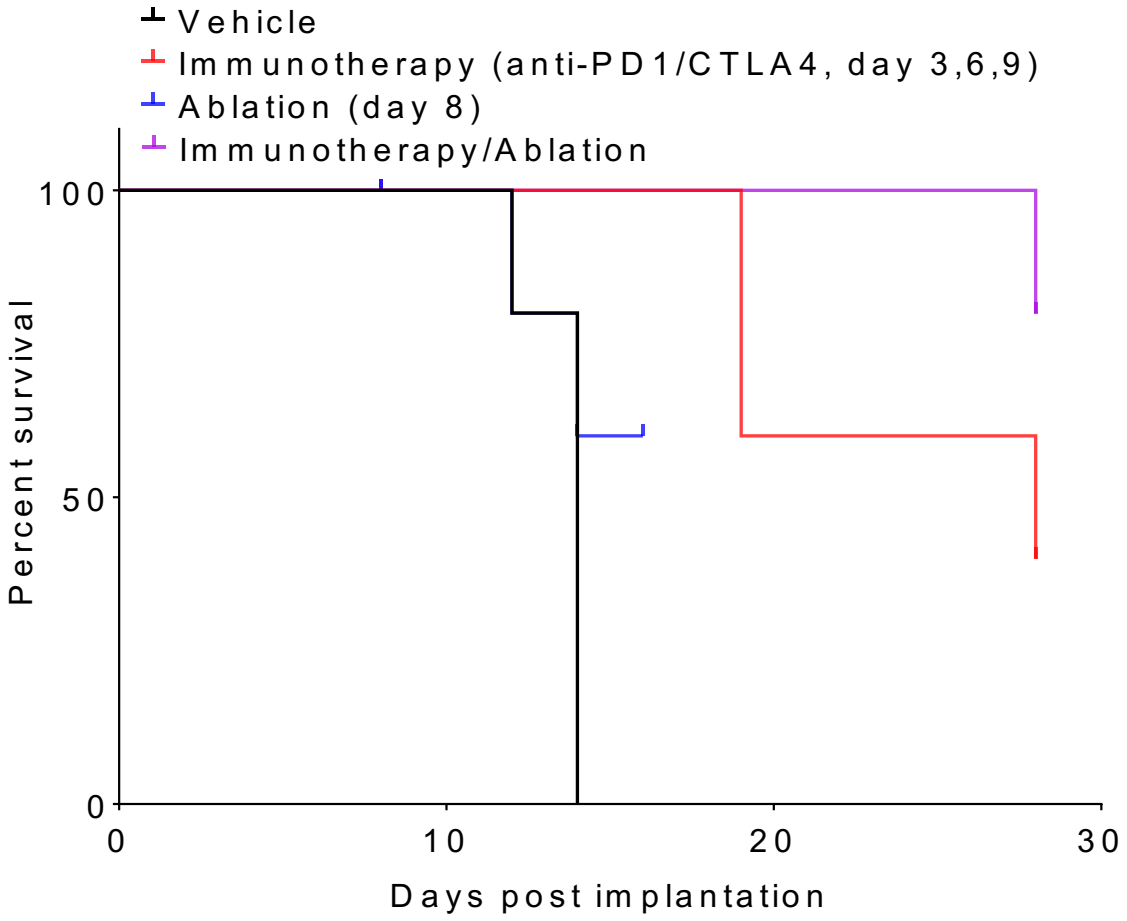

4B) Kaplan-Meier survival plots of MC38 mice with bilateral tumors. Endpoint defined as tumor volume > 750mm^3.

Figure 5: EMT6 bilateral tumor model development to assess immunotherapy and/or cryoablation on tumor growth.

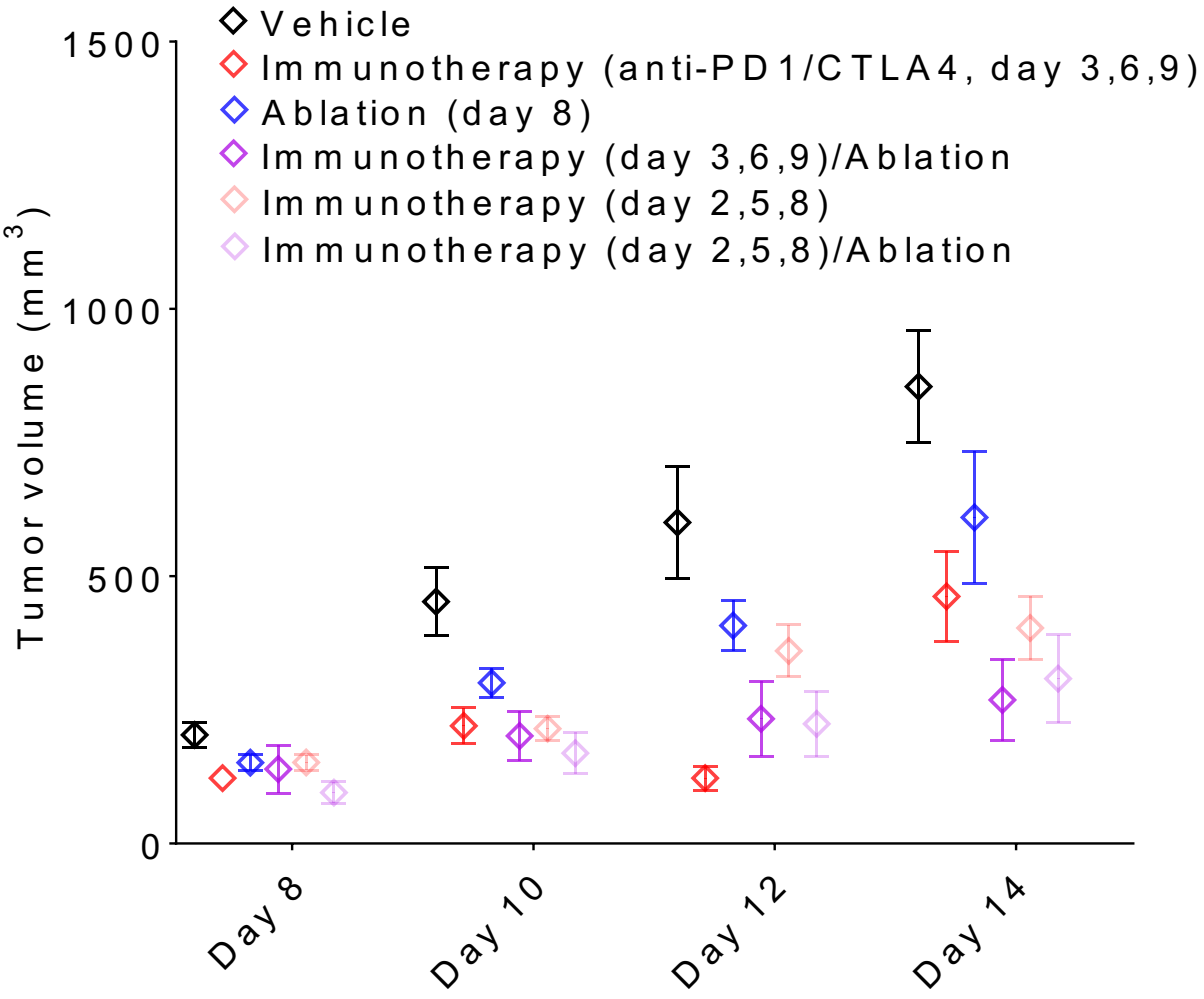

5A) EMT6 growth curves for vehicle (n = 8), immunotherapy (day 3,6,9 n = 7, day 2,5,8 n = 8), ablation (n = 5) and combination (day 3,6,9 n = 8, day 2,5,8 n = 8) groups plotted as mean +/- SEM. P values for vehicle vs IO369 for day 8 (p = 0.01), day 10 (p = 0.01), day 12 (p = 0.001), and day 14 (p = 0.01). P values for vehicle vs ablation for day 8 (p = 0.22), day 10 (p = 0.18), day 12 (p = 0.30), and day 14 (p = 0.22). P values for vehicle vs IO369/ablation for day 8 (p = 0.17), day 10 (p = 0.02), day 12 (p = 0.03), and day 14 (p = 0.002). P values for IO369 vs IO369/ablation for day 8 (p = 0.69), day 10 (p = 0.74), day 12 (p = 0.12), and day 14 (p = 0.12). P values for vehicle vs IO258 for day 8 (p = 0.06), day 10 (p = 0.0009), day 12 (p = 0.04), and day 14 (p = 0.0001). P values for vehicle vs IO258/ablation for day 8 (p = 0.005), day 10 (p = 0.005), day 12 (p = 0.02), and day 14 (p = 0.002). P values for IO258 vs IO/ablation258 for day 8 (p = 0.03), day 10 (p = 0.28), day 12 (p = 0.11), and day 14 (p = 0.35).

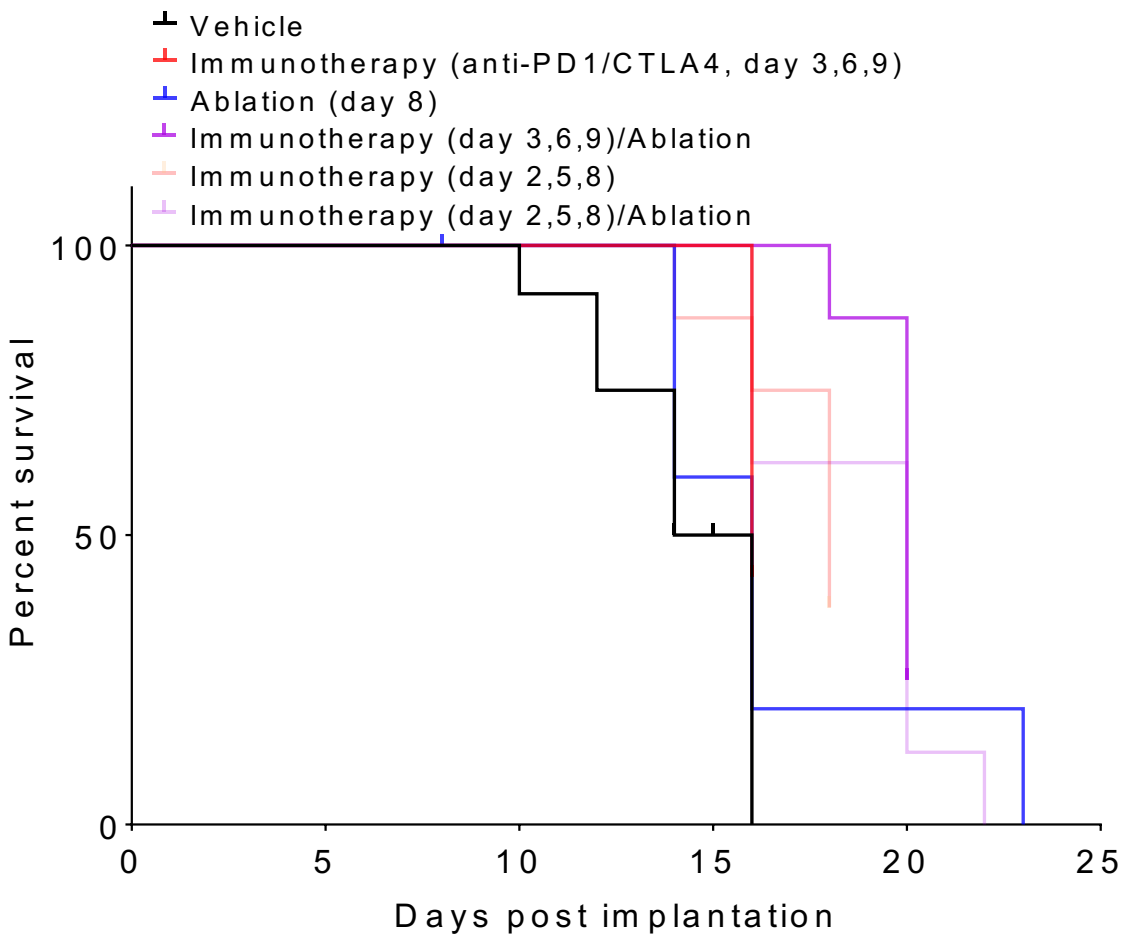

5B) Kaplan-Meier survival plots of EMT6 mice with bilateral tumors. Endpoint defined as tumor volume > 750mm^3. Survival plots subdivided below as vehicle vs all ablation groups, vehicle vs all immunotherapy groups, and immunotherapy vs immunotherapy/ablation groups.

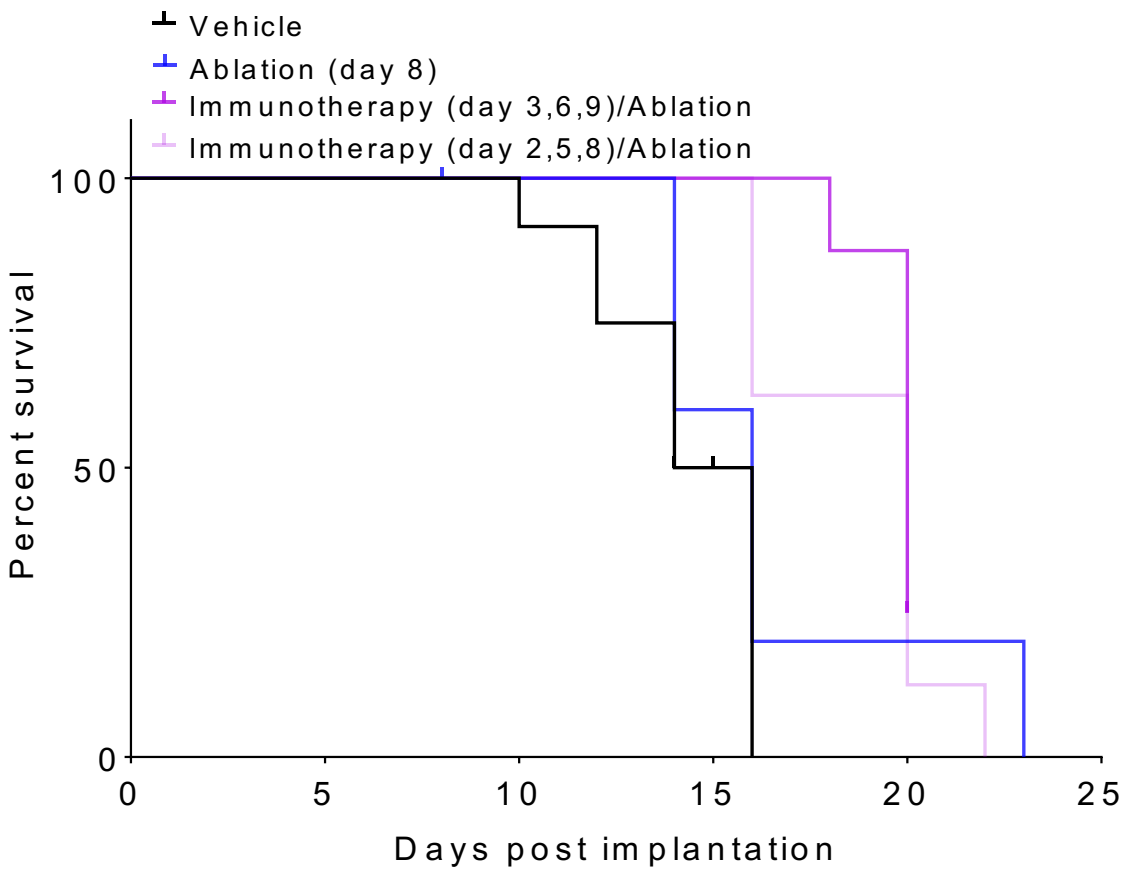
Vehicle
Ablation (day 8)
Immunotherapy (day 3,6,9)/Ablation
Immunotherapy (day 2,5,8)/Ablation
Percent survival
100
50
0
0
5
10
15
20
25
Days post implantation

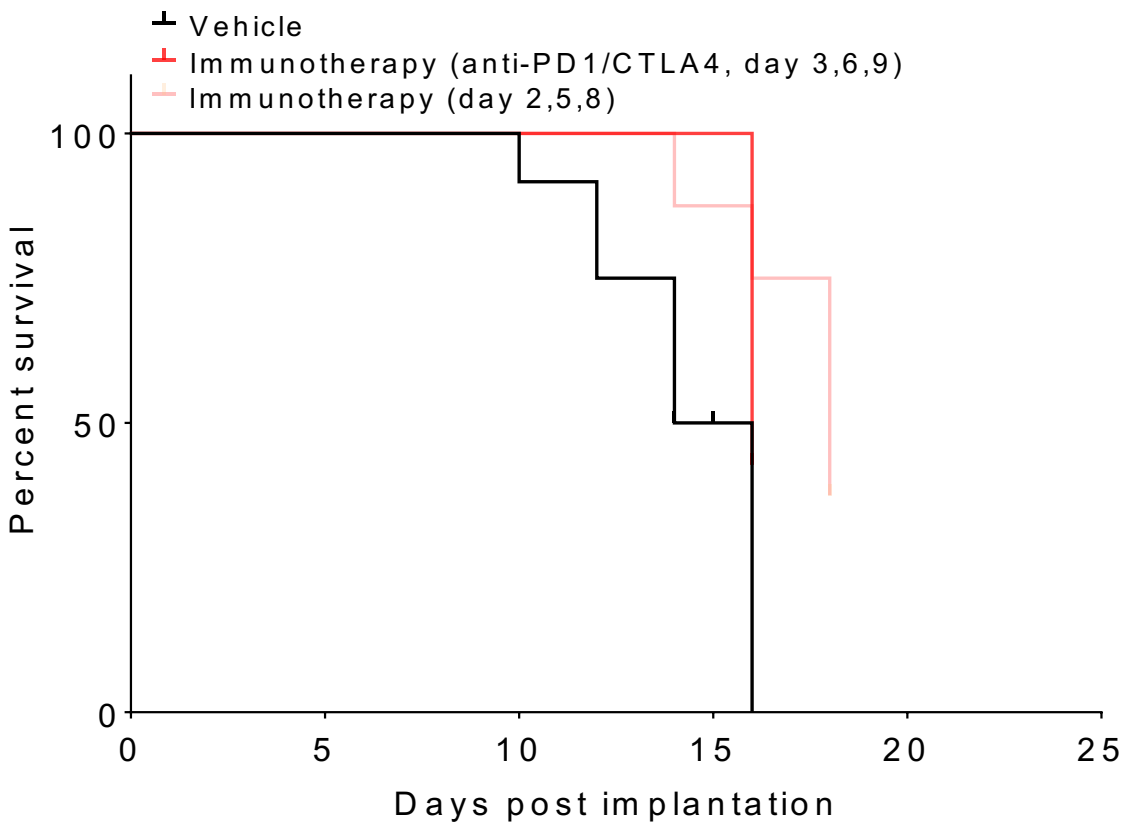
Vehicle
Immunotherapy (anti-PD1/CTLA4, day 3,6,9)
Immunotherapy (day 2,5,8)
Percent survival
100
50
0
0
5
10
15
20
25
Days post implantation

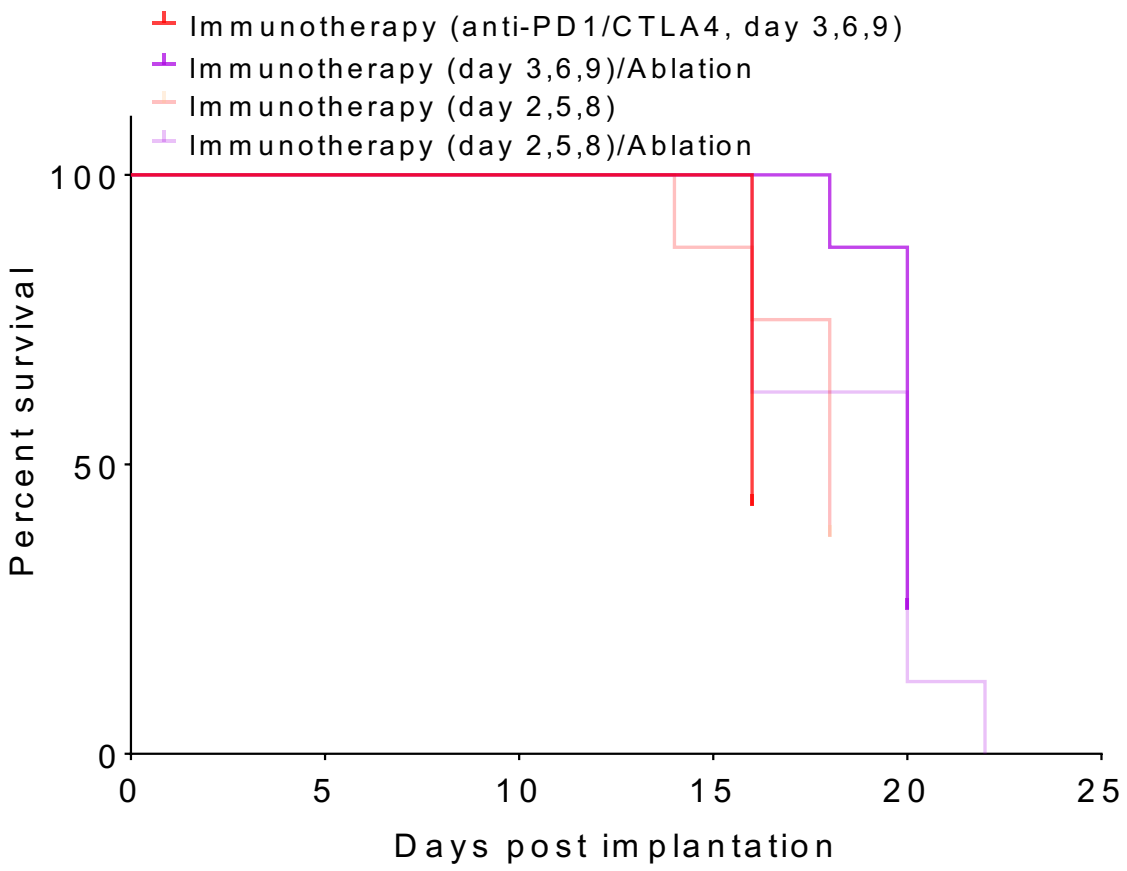
Immunotherapy (anti-PD1/CTLA4, day 3,6,9)
Immunotherapy (day 3,6,9)/Ablation
Immunotherapy (day 2,5,8)
Immunotherapy (day 2,5,8)/Ablation
Percent survival
100
50
0
0
5
10
15
20
25
Days post implantation

Supplemental figures

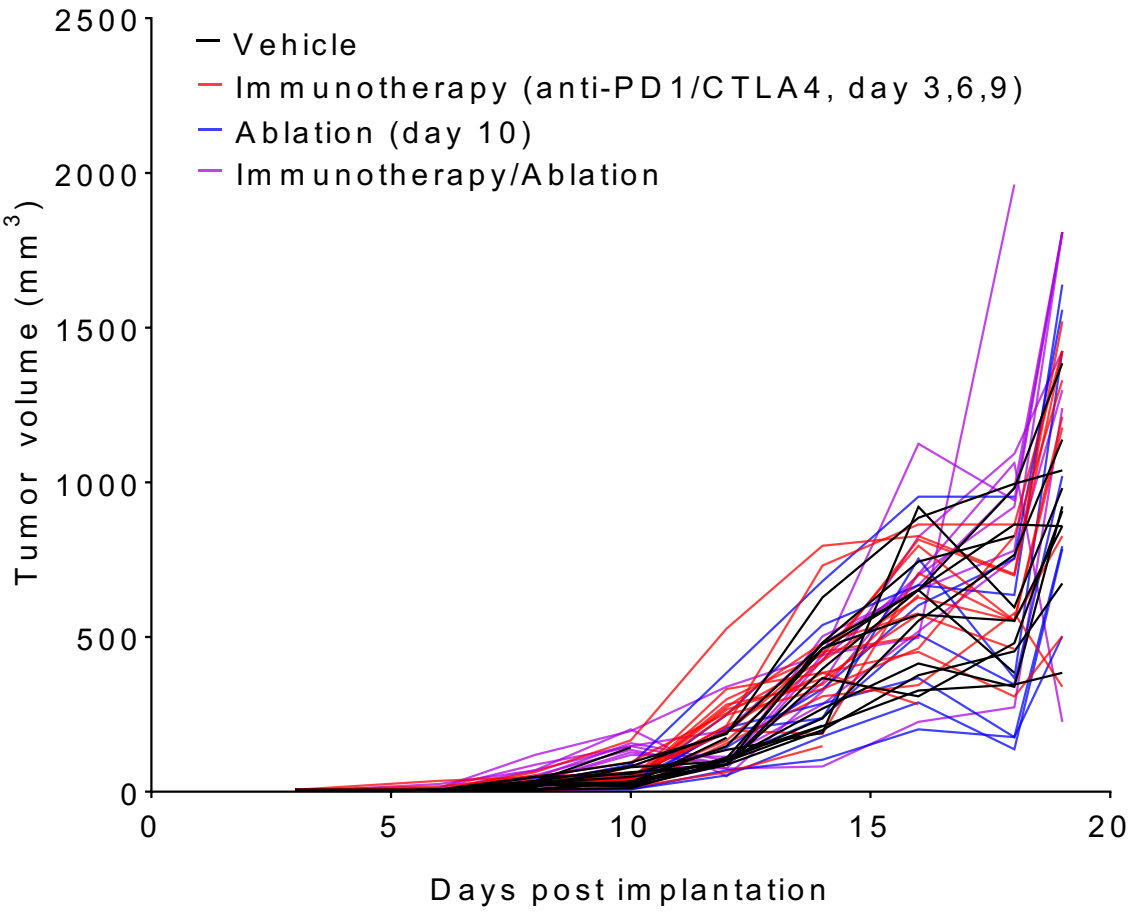

SuppA) LLC1 individual tumor growth curves.

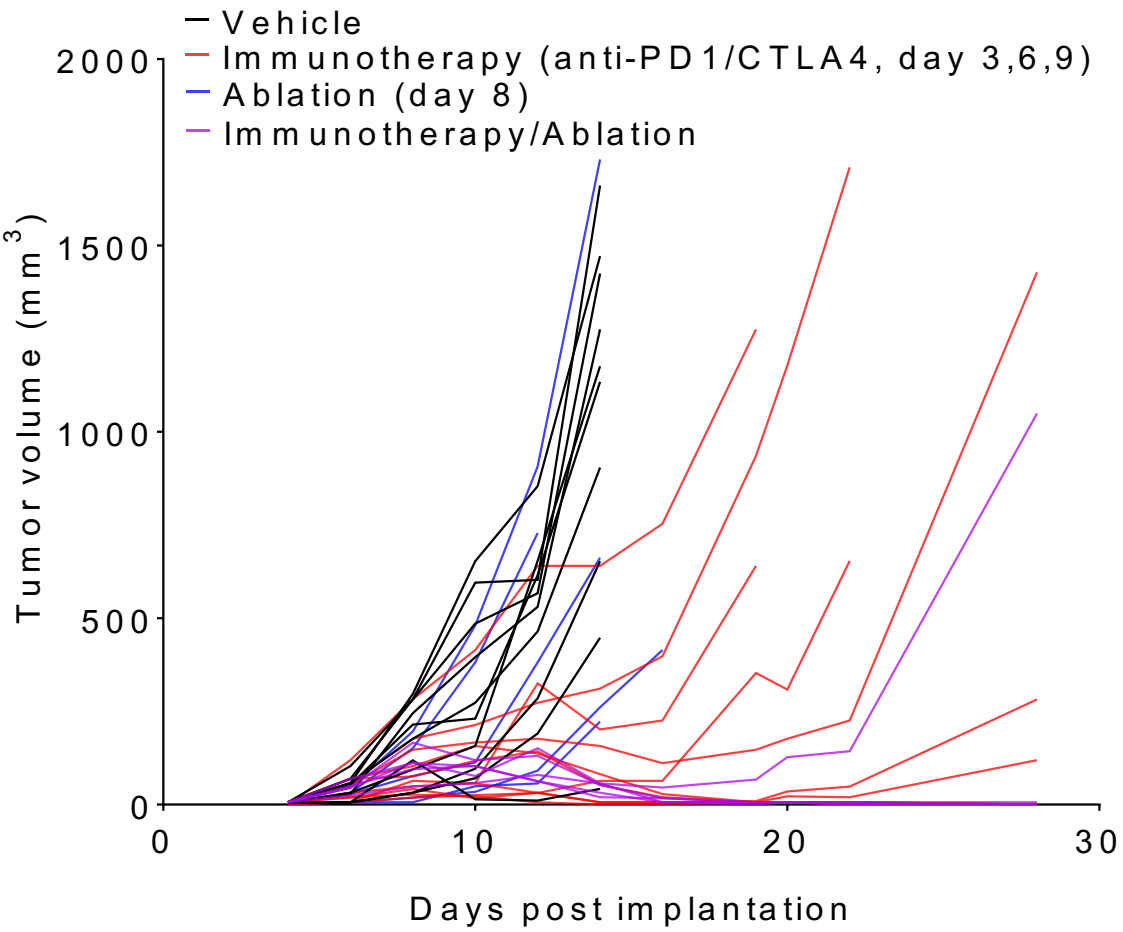

SuppB) MC38 individual tumor growth curves.

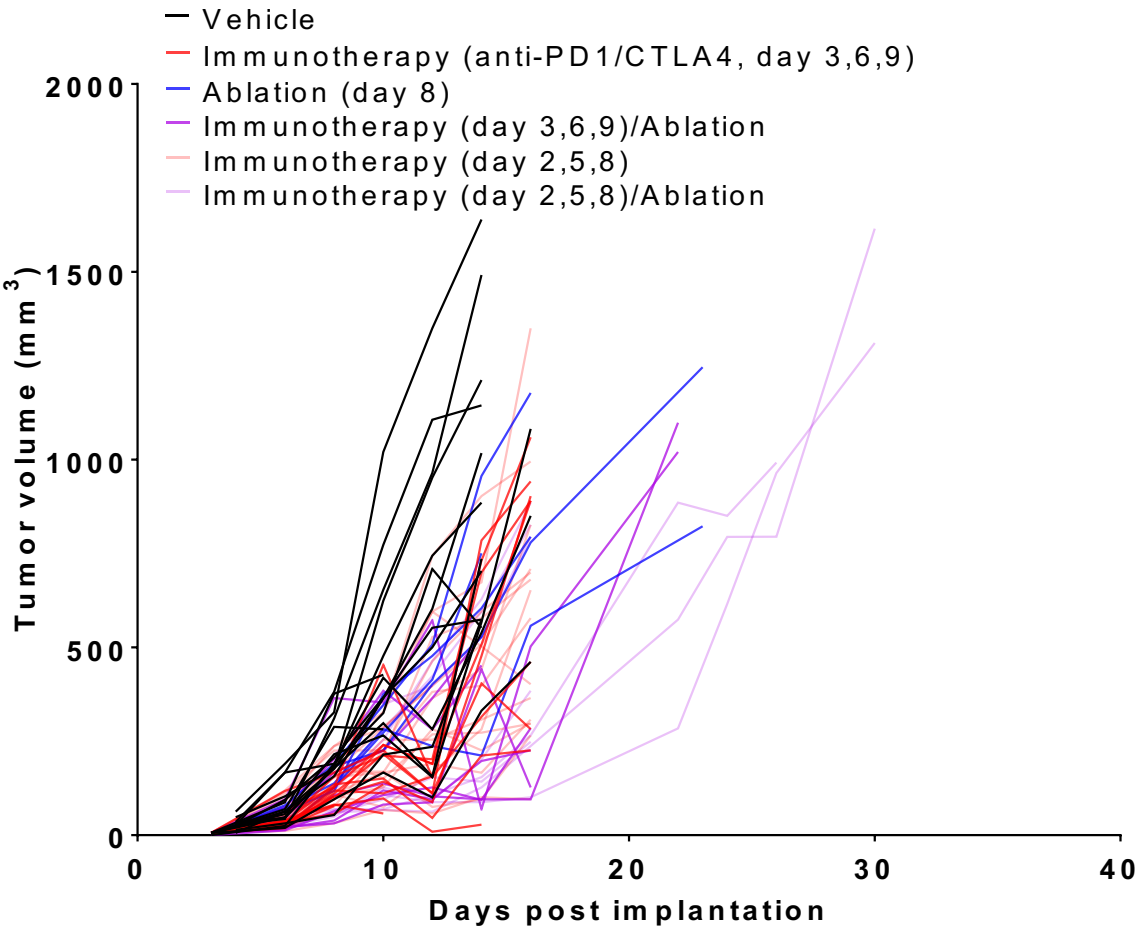

SuppC) EMT6 individual tumor growth curves